J. Earth Syst. Sci. (2021)130 158
https://doi.org/10.1007/s12040-021-01666-3

Ozone chemistry and dynamics at a tropical coastal site impacted by the COVID-19 lockdown

Imran A Girach[1,*], Narendra Ojha[2] and S Suresh Babu[1]

[1]*Space Physics Laboratory, Vikram Sarabhai Space Centre, Thiruvananthapuram 695 022, India.*
[2]*Space and Atmospheric Sciences Division, Physical Research Laboratory, Ahmedabad 380 009, India.*
**Corresponding author. e-mail: imran.girach@gmail.com*

MS received 1 January 2021; revised 17 March 2021; accepted 24 April 2021

The nationwide lockdown in India to curb the spread of Coronavirus disease 2019 (COVID-19) led to colossal reduction in anthropogenic emissions. Here, we investigated the impact of lockdown on surface ozone (O_3) and nitrogen dioxide (NO_2) over a tropical coastal station – Thumba, Thiruvananthapuram (8.5°N, 76.9°E). Daytime as well as night-time NO_2 showed reduction by 0.8 (40%) and 2.3 (35%) ppbv, respectively during the lockdown period of 25–30 March 2020 as compared with the same period of previous 3 years. Unlike many urban locations, daytime surface O_3 is found to be dramatically reduced by 15 ppbv (36%) with O_3 production rate being lower by a factor of 3 during the lockdown. Interestingly, a feature of O_3-hump during the onset of land breeze typically observed during 1997–1998 has reappeared with magnitude of 5–10 ppbv. A photochemical box model, capturing this feature, revealed that significant O_3 sustained till onset of land breeze over the land due to weaker titration with NO_x during lockdown. It is suggested that the transport of this O_3 rich air with onset of land breeze led to the observed hump. Our measurements unravel a remarkable impact of the COVID-19 lockdown on the chemistry and dynamics of O_3 over this tropical coastal environment.

Keywords. Thumba; trace gases; photochemistry; land and sea breeze.

1. Introduction

After the outbreak of Coronavirus disease 2019 (COVID-19) pandemic, lockdowns were imposed in various countries to minimize the spread. The lockdowns have been shown to drastically reduce the anthropogenic emissions improving the air quality significantly (Bauwens *et al.* 2020; Le *et al.* 2020). Large reductions in nitrogen dioxide (NO_2) over major cities have been observed worldwide (Dantas *et al.* 2020; Liu *et al.* 2020). Globally, the reduction in tropospheric O_3 burden by about 6 Tg ($\sim$2%) is suggested to have altered the radiative forcing significantly (Miyazaki *et al.* 2020). The major source of NO_2 is fossil fuel burning in vehicles, industries, power generators, etc. NO_2 is one of the major air pollutants and also the main precursor of ozone (O_3; Seinfeld and Pandis 1998). O_3 plays a key role in tropospheric chemistry as the major source of hydroxyl radical (OH), which is known as detergent for removal of many pollutants from the atmosphere. O_3 also controls the oxidation capacity of the troposphere, besides its role as a greenhouse gas. O_3 is not directly emitted in the

Supplementary material pertaining to this article is available on the *Journal of Earth System Science* website (http://www.ias.ac.in/Journals/Journal_of_Earth_System_Science).

Published online: 09 August 2021

atmosphere, rather it is formed through photochemical reactions, involving the precursor gases such as nitrogen oxides (NO_x = NO + NO_2), CO, and hydrocarbons (Seinfeld and Pandis 1998). Two competing chemical processes, O_3 production via photolysis of NO_2 *vs.* O_3 destruction by NO, govern O_3 variability in urban and rural environments. While higher O_3 levels during daytime are due to dominance of photochemical production, the titration reaction dominates during night-time causing lower O_3 levels (Seinfeld and Pandis 1998). Nevertheless, the dependence of O_3 on the concentrations of the precursors is complex and non-linear. Therefore, accurate measurements over distinct environment are necessary to characterise the chemical regimes and to understand role of various atmospheric processes.

A nationwide lockdown was also imposed by the Government of India starting since 25 March 2020 (https://mha.gov.in/sites/default/files/PR_NationalLockdown_26032020_0.pdf). A 14-hr voluntary 'Janata (i.e., public) curfew' was also observed on 22 March 2020. The lockdown was implemented in a phased manner, during phase-1 (25 March–14 April 2020) and phase-2 (15 April–03 May 2020), the imposed guidelines restricted movements of all vehicles, industrial activities, and other services, except the essential and emergency services. Thus, anthropogenic emissions of trace gases and aerosols from various sources such as vehicles, industries, etc., largely came to a halt. Since phase-3 (04 May 2020 onwards), certain relaxations were implemented which included vehicular movements and a few other anthropogenic activities. However, lockdown restrictions remained stringent over the hotspot regions (https://www.mha.gov.in/notifications/circulars-covid-19). Recently, a few studies have reported the reduction of air pollutants near source regions over megacities in India (Kumari and Toshniwal 2020; Mahato *et al.* 2020; Sharma *et al.* 2020) and synoptic changes over the Indian region (Shehzad *et al.* 2020). Black carbon concentrations showed reductions in the range of 16–60% with respect to climatological mean over the Indian region (Gogoi *et al.* 2021). Observations from 134 monitoring sites of Central Pollution Control Board across India showed reduction of ∼40–70% in $PM_{2.5}$, ∼40–60% in PM_{10}; ∼30–70% in NO_2; and ∼20–40% in CO, but the changes in surface O_3 were observed to be site-specific (Dhaka *et al.* 2020; Singh *et al.* 2020; Soni *et al.* 2021). However, O_3 chemistry over tropical coastal environments away from strong sources but impacted by land–sea breeze systems, has not yet been explored. In this regard, we have investigated the changes in surface O_3 as well as NO_2 over a tropical coastal station by analysing *in-situ* measurements during the first week of lockdown (25–30 March 2020). In addition, measurements available over India's capital, Delhi (28.7°N, 77.1°E) were used to infer the heterogeneity in surface O_3 chemistry.

2. Experimental site, instrumentation and data

The observational site Thumba, Thiruvananthapuram (8.5°N, 76.9°E, ∼3 m amsl), is situated on the southwest coast of India, approximately 500 m away from the Arabian Sea coast. This tropical coastal site experiences typical mesoscale circulation comprising of sea-breeze (SB) during daytime and land-breeze (LB) during night-time almost throughout the year (Narayanan 1967). Thiruvananthapuram district has a population of 3.3 million as per census 2011.

In-situ measurements of surface O_3 and NO_x were performed using ultraviolet (UV) photometric O_3 analyser (model 49 C) and chemiluminescence NO_x analyser (Model 42i) of Thermo Electron Corporation, USA, respectively. Based on absorption of UV radiation at ∼253.7 nm by O_3 molecules, O_3 mixing ratios in sample air were derived using the Beer–Lambert law. NO_x analyser works on the principle of chemiluminescence property of NO_2 molecules. The oxidation of NO by O_3 molecules forms excited NO_2 molecules. The measurement of luminous radiation emitted by these excited NO_2 molecules is a measure of NO concentration. NO_2 is measured by converting it into NO using molybdenum converter under high temperature. Sample air was drawn from ∼3 m above the ground using a Teflon tube and pre-conditioned air (dehumidified and filtered for dust particles) was fed to the analysers for these measurements. O_3 analyser was calibrated with an in-built O_3 generator and a zero air generator. The uncertainty in O_3 mixing ratio, lower detection limit, and linearity are ±5%, 1 ppbv and 1%, respectively. NO_x analyser was calibrated using standards traceable to the National Institute of Standards and Technology diluted with custom-made calibrator. Lower detection limit, linearity, and uncertainty for NO_x measurements are 0.05 ppbv, 1% and ±5%, respectively (Tanimoto *et al.* 2007). Data were recorded at 5 min intervals. Further details of instruments as well as site description can be found

elsewhere (Girach *et al.* 2012; Nair *et al.* 2018). The observations during 25–30 March 2020 (6 days), besides observations during pre-lockdown period and previous years are used in the present study.

In addition, surface wind speed and direction used in the study were measured using the automatic weather station (AWS), Dynalab Weathertech Pvt. Ltd, India, having accuracy of ±0.5 ms^{-1} and ±3°, respectively.

For the purpose of comparison of O_3 changes, measurements at 14 different sites across Delhi (28.7°N; 77.1°E) made under the National Air Quality Monitoring Programme (NAMP) by Central Pollution Control Board (CPCB) under Ministry of Environment, Forest and Climate Change (MoEFCC) of India are also used. Hourly averaged O_3 data falling beyond 3-sigma standard deviations were filtered prior to estimation of daily averages. Details on measurements and filtering criteria can be found in the CPCB reports (CPCB 2011) and previous studies (Schnell *et al.* 2018).

3. Results and discussions

Diurnal patterns of surface O_3 is characterised by higher mixing ratios during daytime and lower mixing ratios during night-time, opposite to NO_2 diurnal variations, over Thumba. These variations in O_3 and NO_2 are significantly influenced by photochemistry, SB and LB activity, besides the impact of boundary layer changes (Nair *et al.* 2002; David and Nair 2011; Girach *et al.* 2012). Daytime (12–17 hrs) and night-time (23–06 hrs) average NO_2 variations are shown in figure 1 during 19–30 March 2020 and during the same period of previous 3 years (during 2016–2019). Generally, night-time NO_2 level is higher than that of daytime (figure 1) due to absence of NO_2 photolysis, titration of O_3 with NO producing NO_2, shallow boundary layer height limiting the vertical mixing, and prevalence of LB transporting NO_x rich air to the study site (David and Nair 2011; Girach *et al.* 2012). Daytime NO_2 during Janata curfew day showed some reduction, and daytime NO_2 value of the previous day is comparable to that of the mean value of this day of previous years. However, reduction in night-time NO_2 was beyond 1-sigma variability due to reduced emission during daytime under the curfew restrictions. A quick response to reduction in emission is mainly due to a shorter lifetime of NO_2 (2–8 hrs; Liu *et al.* 2016). Although unexpected, NO_2 remained lower on subsequent day. Daytime

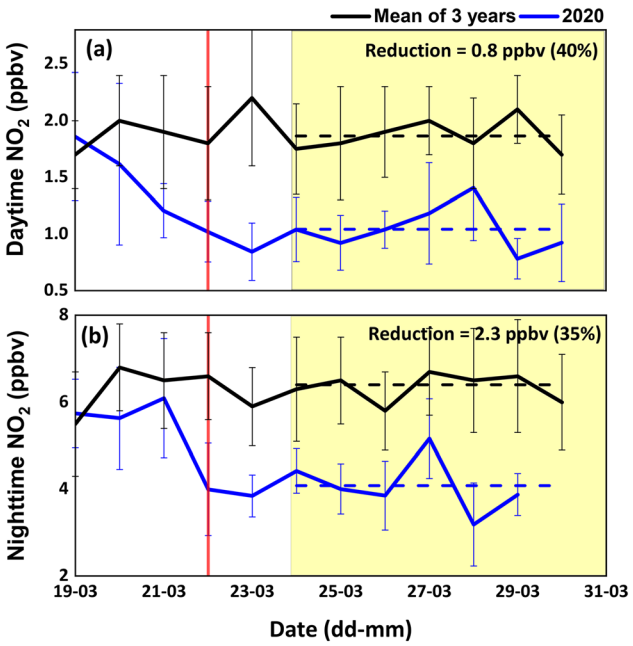

Figure 1. Mean daytime **(a)** and night-time **(b)** NO_2 during lockdown period of 2020 and during the same period of previous 3 years. Error bars represent standard deviations. Red line, yellow shaded region, dashed line mark the 'Janata curfew' day, lockdown period and mean over lockdown period, respectively.

and night-time NO_2 during lockdown period of 25–30 March 2020 were observed to be significantly lower (beyond 1-sigma standard deviation) with respect to mean values in previous years. Average values during this period are shown by horizontal dashed lines in figure 1. While NO_2 was reduced by 0.8 ppbv (40%) during daytime, reduction during night-time is seen to be 2.3 ppbv (35%). Larger reduction in absolute magnitude of night-time NO_2 is expected as LB transports the relatively polluted airmass from the land. Since night-time NO_2 levels are associated with daytime O_3 (David and Nair 2011), impact on daytime O_3 is expected to be significant as discussed subsequently. The observations from Tropospheric Monitoring Instrument (TROPOMI) aboard Sentinel-5 Precursor satellite showed $1.0\times10^{15} \pm 3.0\times10^{14}$ molecules cm^{-2} tropospheric NO_2 during 24–30 March 2020 over the study location, which was lower by ∼40% as compared to the level ($1.7\times10^{15} \pm 1.3\times10^{14}$ molecules cm^{-2}) during same period of previous year. This reduction was also beyond the 1-sigma standard deviation and in line with the percentage reduction seen in daytime surface NO_2.

Figure 2(a) shows the daytime O_3 during lockdown period (yellow shaded region) and the same period of previous years. Daytime O_3 showed

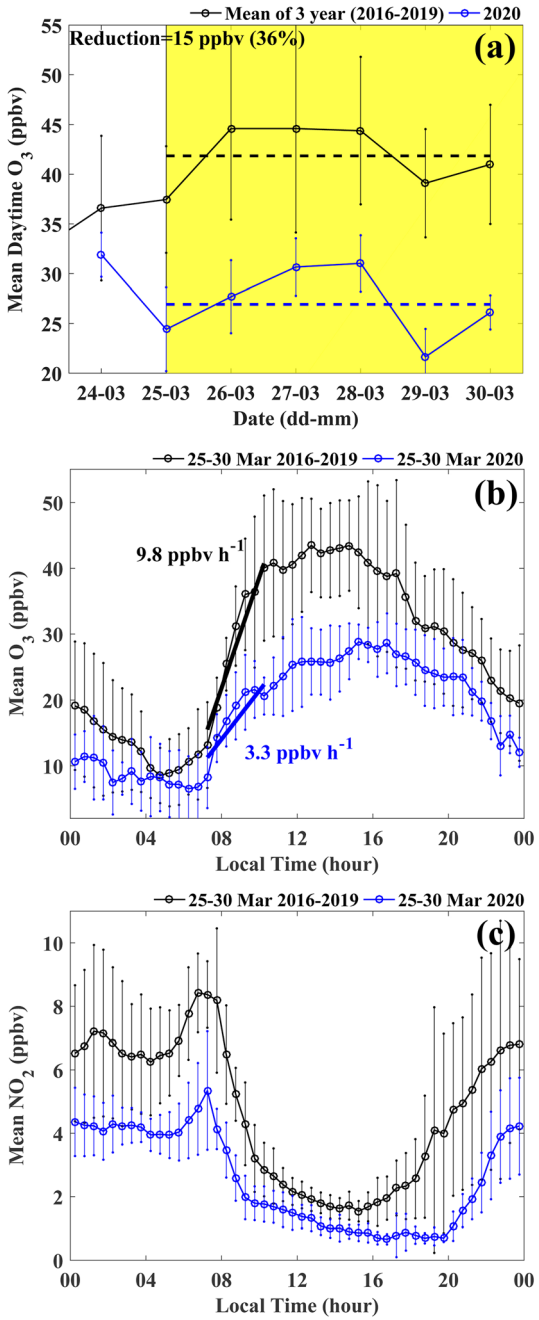

Figure 2. Mean daytime O_3 **(a)**, diurnal variation of O_3 **(b)**, and NO_2 **(c)** during lockdown period of 2020 and during the same period of previous 3 years. Error bars represent standard deviations. Yellow shaded region and dashed line in (a) denote the lockdown period and mean over lockdown period, respectively. Thick black and blue lines in (b) represent the linear fits for the morning hours (07–10 hr).

reduction by 15 ppbv (36%), however, small reduction of ∼4 ppbv in night-time O_3 was not significant (within standard deviation; see supplementary figure S1). These observations of daytime O_3 reduction are in contrast with studies from other urban environments showing daytime enhancement (Resmi *et al.* 2020; Soni *et al.* 2020; Panda *et al.* 2021). Figure 2(b) shows the mean diurnal variations of O_3 where suppression in O_3 production is clearly evident during lockdown period. Considering the O_3 during morning hours (07–10 hrs), estimated slope from linear regression analysis is a measure of O_3 production rate. O_3 production rate which was 9.8 ppbv h^{-1} during previous years is found to be reduced to 3.3 ppbv h^{-1}, i.e., by a factor of 3 during the lockdown. Figure 2(c) shows the mean diurnal variations of NO_2 where effective suppression of fumigation peak during morning hours is clearly evident, besides lower values during day and night. Since O_3 production rate depends on precursor concentrations, lower levels of NO_2 (and other precursors) in the morning hours (figure 2c) could result in reduced production rate and lower daytime O_3. It is worth to mention here that NO_2 dispersed over the sea during LB (night-time) gets recirculated, after chemical losses, during SB which prevails during daytime over the site (David and Nair 2011). Lower NO_x during night could have enhanced O_3 by reducing its titration with NO during night-time (23–06 hrs). However, since O_3 level itself was reduced during daytime, influence of reduced titration is compensated and significant change in night-time O_3 was not observed. However, the slower evening loss in O_3 was observed as discussed subsequently.

SB component (SBC) is calculated as [wind speed × sin(325° – wind direction)] as the coastline of Thiruvananthapuram is aligned along ∼145–325°. Figure 3 shows diurnal variations of O_3 for three individual days (25–27 March 2020) along with SB component. SBC is used to demarcate SB and LB, as positive and negative values denote SB and LB, respectively. Crossing from SB to LB denote the onset of LB as marked by red dashed line in figure 3. In normal conditions, it has already been illustrated that O_3 remains high till the onset of LB (David and Nair 2011; Girach *et al.* 2012). O_3 started decreasing with reduction in solar radiation (sunset time is marked with black dashed line in figure 3). Interestingly, a hump of 5–10 ppbv around the LB onset is observed over three days. This feature was observed consistently during 1997–1998 over the site as reported by Nair *et al.* (2002). However, it has not been observed regularly in the recent years, as reported by David and Nair (2011).

In order to explain the O_3-hump with onset of LB, we have performed simulations using a photochemical box model. We used Master Mechanism

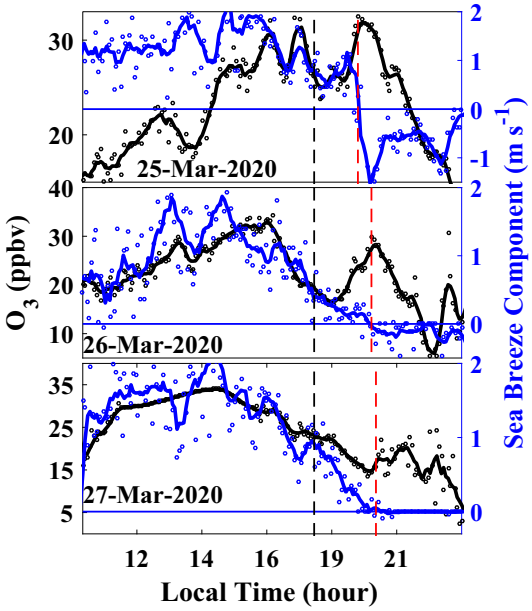

Figure 3. Diurnal variations of O_3 (black) and sea breeze component for 3 days during lockdown period. Black and red dashed lines represent sunset time and onset of land breeze, respectively.

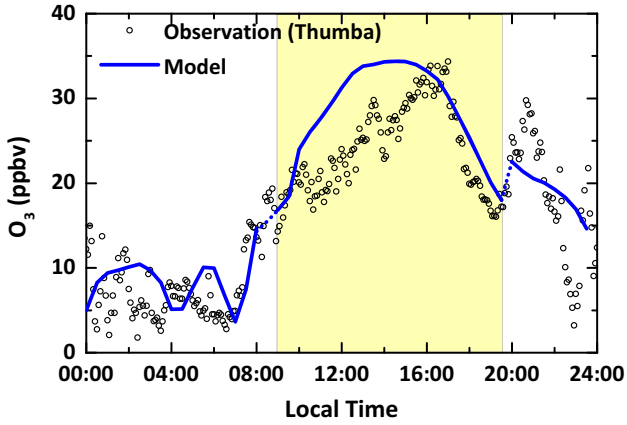

Figure 4. Observed and model simulated diurnal variation of surface O_3 on 26 March 2020. Yellow shaded region demark the SB airmass. Blue dots connect O_3 simulated for airmasses over land and sea.

model – version 2.5, developed at National Center for Atmospheric Research (NCAR), which simulates chemical evolution of air parcel with time considering the detailed photochemistry in absence of dynamics or further emissions. The detailed description of the model can be found elsewhere (Madronich 2006; Nair *et al.* 2011; Ojha *et al.* 2012; Soni *et al.* 2021). The environmental conditions such as latitude, longitude, date, parcel elevation, total column ozone, SO_2 column, NO_2 column, aerosol optical depth, single scattering albedo, aerosol angstrom coefficient, temperature, air density were set to typical values of 8.5°N, 76.9°E, 26 March 2020, 10 m, 280 DU, 0.12 DU, 0.11 DU, 0.50, 0.82, 1.2, 300 K, 2.45×10^{19} molecules cm^{-3}, respectively as obtained from Ozone Monitoring Instrument (https://disc.gsfc.nasa.gov/), ground-based observations at the study site and literature (Babu *et al.* 2007; David and Nair 2011). The initial/background concentrations of carbon monoxide, methane, isoprene, formaldehyde, ethane, ethene, propane, propene, *n*-butane, and *i*-butane were included as 300, 2000, 1, 0.7, 2.5, 5, 1.5, 3, 5, and 0.1 ppbv, respectively, which represent the typical coastal/rural conditions. The background value of O_3 has been set as free tropospheric value of 40 ppbv (Ajayakumar *et al.* 2019). The crucial diurnal constraints used in the simulation were the observed nitric oxide (NO) and NO_2 (supplementary figure S2). In order to account for the overestimation in the measurement of NO_2 due to molybdenum convertor (Winer *et al.* 1974), observed NO_2 were used in the simulation after giving an offset of 35% based on sensitivity simulations. In addition, variation of boundary layer height and entrainment velocity were assumed to their typical values of 0.2–1.5 km and 0.05–20 cm s^{-1}, respectively (Bremaud *et al.* 1998; Girach *et al.* 2012).

We performed first simulation for airmasses sampled at Thumba site based on above-mentioned model configuration. As SB airmass travels over the land during daytime, it gets enriched by precursors (i.e., NO_2) due to, for instance, vehicular emission. Thus, by giving a small increment of 35% in NO_2, we performed another simulation for airmasses over land. As Thumba site experiences airmasses from land during night-time, we have combined the two simulations in figure 4. The model reproduced the observed diurnal feature of O_3, including the O_3-hump around onset of LB. However, magnitude of simulated O_3-hump is ∼5 ppbv, smaller than the observed value, which could be partly due to discount of transport. Diurnal variation of O_3 simulated for the airmass over land showed higher levels of O_3 during daytime, which is in agreement with the observations at an inland station Kariavattom (8.56°N; 76.89°E, ∼4 km from the coast), which is close to Thumba (supplementary figures S3 and S4). Significant O_3 level sustained in the evening hours due to lower NO caused by reduced emission under lockdown. This slow losses of O_3 after sunset, results in significant O_3 even in evening hours, similar to that over a rural site in India (Naja and Lal 2002). Thus, in nutshell, this feature of O_3-hump is attributed to

the weaker O_3 titration with NO over land during lockdown. This allowed a significant amount of O_3 to sustain over land and get transported to the observational site with the onset of LB.

It is worth mentioning that under normal condition (unlike lockdown), higher NO in the evening hours titrates O_3 effectively after sunset and O_3 levels in the LB are much lower and hence O_3-hump is not seen under normal condition. The above mechanism would also explain the O_3-hump reported earlier (Nair *et al.* 2002) due to lower NO_x at that time (Nair *et al.* 2018).

To compare the O_3 behaviour in a contrasting environment, we utilised the O_3 observations over NO_x-rich environment, Delhi. Figure 5 shows the daytime O_3 averaged over 14 monitoring stations across Delhi during lockdown period of 25 March–04 April 2020. After the implementation of lockdown surface O_3 showed reduction by ∼25 ppbv; however, after a few days, O_3 started increasing slowly converging to reference curve of 2019 afterwards. The increase in O_3 across Delhi (Mahato *et al.* 2020) and over another urban location, Ahmedabad (Soni *et al.* 2021) was mainly attributed to stronger diminish of NO which titrates O_3, non-linear chemistry and changes in meteorology. Thus, overall daytime O_3 reduction is insignificant over Delhi specifically few days after lockdown. This feature shows the non-linear and complex O_3 chemistry for urban locations where plenty of volatile organic compounds are present besides heterogeneous chemistry under significant aerosol loading. This also points to the contrasting behaviour of chemistry and dynamics of O_3 as observed over a coastal station.

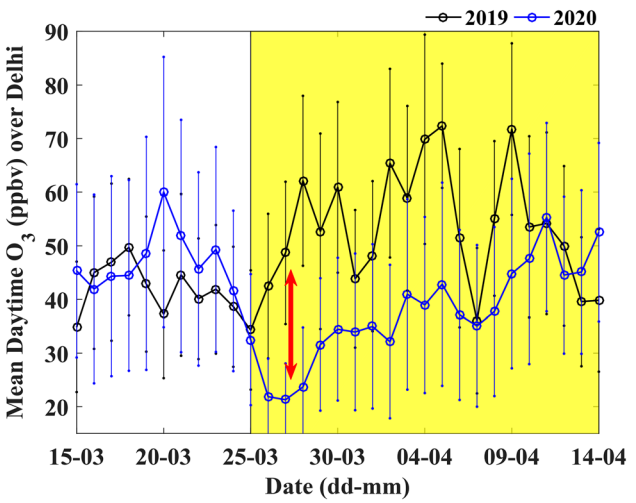

Figure 5. Mean daytime O_3 over Delhi during lockdown period of 2020 and during the same period of 2019. Error bars represent standard deviations. Yellow shaded region and red arrow denote the lockdown period and O_3 reduction during the initial days of lockdown, respectively.

4. Summary and conclusions

Present study highlights the impact of lockdown on surface O_3 chemistry over a tropical coastal station, Thiruvananthapuram, during first week of lockdown (25–30 March 2020). O_3 precursor, NO_2 reduced significantly (2.3 and 0.8 ppbv during night-time and daytime, respectively) which led to suppression of observed O_3 production rate by a factor of 3. Suppression of fumigation peak in NO_2 contributed in lowering the O_3 production rate. Consequently, daytime (12–17 hrs) surface O_3 reduction of 15 ppbv (36%) was seen. Interestingly, surface O_3 showed a hump (5–10 ppbv) around the onset of land breeze. The O_3-hump was reproduced by the simulations using a photochemical box model. Reappearance of this feature which was seen during 1997–1998, is due to a weaker titration slowing the evening time O_3 losses over the land and sustaining significant O_3 levels till the onset of land breeze. This study shows that the lockdown has influenced the O_3 chemistry and dynamics dramatically over this tropical coastal region.

Acknowledgements

We gratefully acknowledge the Central Pollution Control Board, Ministry of Environment, Forest and Climate Change (MoEFCC) for the ground-based measurement of O_3 over Delhi obtained from website, https://app.cpcbccr.com/ccr/#/caaqm-dashboard/caaqm-landing. We thank S Madronich and co-workers for freely available Master Mechanism model through the website of NCAR ACOM. We also acknowledge the use of tropospheric NO_2 column data from the TROPOMI as obtained from https://disc.gsfc.nasa.gov/datasets?keywords=tropomi%20no2&page=1. Constructive comments and suggestions from two anonymous reviewers are acknowledged.

Author statement

Imran A Girach: Conceptualization, measurements, analysis, modelling, manuscript preparation; Narendra Ojha: analysis, visualisation, writing, review & editing; S Suresh Babu: guidance and supervision.

References

Ajayakumar R S, Nair P R, Girach I A, Sunilkumar S V, Muhsin M and Satheesh Chandran P R 2019 Dynamical nature of tropospheric ozone over a tropical location in Peninsular India: Role of transport and water vapour; *Atmos. Environ.* **218**, https://doi.org/10.1016/j.atmosenv.2019.117018.

Babu S S, Moorthy K K and Satheesh S K 2007 Temporal heterogeneity in aerosol characteristics and the resulting radiative impacts at a tropical coastal station – Part 2: Direct short wave radiative forcing; *Ann. Geophys.* **25** 2309–2320, https://doi.org/10.5194/angeo-25-2309-2007.

Bauwens M, Compernolle S, Stavrakou T, Müller J-F, van Gent J, Eskes H, Levelt P F, van der A R, Veefkind J P, Vlietinck J, Yu H and Zehner C 2020 Impact of coronavirus outbreak on NO_2 pollution assessed using TROPOMI and OMI observations; *Geophys. Res. Lett.* **47** e2020GL087978, https://doi.org/10.1029/2020GL087978.

Bremaud P J, Taupin F, Thompson A M and Chaumerliac N 1998 Ozone nighttime recovery in the marine boundary layer: Measurement and simulation of the ozone diurnal cycle at Reunion Island; *J. Geophys. Res.* **103** 3463–3473, https://doi.org/10.1029/97JD01972.

Dantas G, Siciliano B, França B B, da Silva C M and Arbilla G 2020 The impact of COVID-19 partial lockdown on the air quality of the city of Rio de Janeiro, Brazil; *Sci. Total Environ.* **729** 139085, https://doi.org/10.1016/j.scitotenv.2020.139085.

David L M and Nair P R 2011 Diurnal and seasonal variability of surface ozone and NO_x at a tropical coastal site: Association with mesoscale and synoptic meteorological conditions; *J. Geophys. Res.* **116**, https://doi.org/10.1029/2010JD015076.

Dhaka S K, Chetna Kumar V, Panwar V, Dimri A P, Singh N, Patra P K, Matsumi Y, Takigawa M, Nakayama T, Yamaji K, Kajino M, Misra P and Hayashida S 2020 PM2.5 diminution and haze events over Delhi during the COVID-19 lockdown period: An interplay between the baseline pollution and meteorology; *Sci. Rep.* **10** 13442, https://doi.org/10.1038/s41598-020-70179-8.

Girach I A, Nair P R, David L M, Hegde P, Mishra M K, Kumar G M, Das S M, Ojha N and Naja M 2012 The changes in near-surface ozone and precursors at two nearby tropical sites during annular solar eclipse of 15 January 2010; *J. Geophys. Res.* **117**, https://doi.org/10.1029/2011JD016521.

Gogoi M M, Babu S S, Arun B S, Moorthy K K, Ajay A, Ajay P, Suryavanshi A, Borgohain A, Guha A, Shaikh A, Pathak B, Gharai B, Ramasamy B, Balakrishnaiah G, Menon H B, Kuniyal J C, Krishnan J, RamaGopal K, Maheswari M, Naja M, Kaur P, Bhuyan P K, Gupta P, Singh P, Srivastava P, Singh R S, Rastogi S, Kundu S S, Kompalli S K, Panda S, Rao T C, Das T and Kant Y 2021 Response of ambient BC concentration across the Indian region to the nation-wide lockdown: Results from the ARFINET measurements of ISRO-GBP; *Curr. Sci.* **120** 341–351.

Kumari P and Toshniwal D 2020 Impact of lockdown measures during COVID-19 on air quality: A case study of India; *Int; J. Environ. Health Res.* **1–8**, https://doi.org/10.1080/09603123.2020.1778646.

Le T, Wang Y, Liu L, Yang J, Yung Y L, Li G and Seinfeld J H 2020 Unexpected air pollution with marked emission reductions during the COVID-19 outbreak in China; *Science* **369** 702–706, https://doi.org/10.1126/science.abb7431.

Liu F, Beirle S, Zhang Q, Dörner S, He K and Wagner T 2016 NO_x lifetimes and emissions of cities and power plants in polluted background estimated by satellite observations; *Atmos. Chem. Phys.* **16** 5283–5298, https://doi.org/10.5194/acp-16-5283-2016.

Liu F, Page A, Strode S A, Yoshida Y, Choi S, Zheng B, Lamsal L N, Li C, Krotkov N A, Eskes H, van der A R, Veefkind P, Levelt P F, Hauser O P and Joiner J 2020 Abrupt decline in tropospheric nitrogen dioxide over China after the outbreak of COVID-19; *Sci. Adv.* **6** eabc2992, https://doi.org/10.1126/sciadv.abc2992.

Madronich S 2006 Chemical evolution of gaseous air pollutants down-wind of tropical megacities: Mexico City case study; *Atmos. Environ.* **40** 6012–6018, https://doi.org/10.1016/j.atmosenv.2005.08.047.

Mahato S, Pal S and Ghosh K G 2020 Effect of lockdown amid COVID-19 pandemic on air quality of the megacity Delhi, India; *Sci. Total Environ.* **730** 139086, https://doi.org/10.1016/j.scitotenv.2020.139086.

Miyazaki K, Bowman K, Sekiya T, Takigawa M, Neu J L, Sudo K, Osterman G and Eskes H 2020 Global tropospheric ozone responses to reduced NOx emissions linked to the COVID-19 world-wide lockdowns; *Earth and Space Science Open Archive ESSOAr* **3** 1–37, https://doi.org/10.1002/essoar.10504795.1.

Nair P R, Ajayakumar R S, David L M, Girach I A and Mottungan K 2018 Decadal changes in surface ozone at the tropical station Thiruvananthapuram (8.542°N, 76.858°E), India: Effects of anthropogenic activities and meteorological variability; *Environ. Sci. Pollut. Res.* **25**, https://doi.org/10.1007/s11356-018-1695-x.

Nair P R, Chand D, Lal S, Modh K S, Naja M, Parameswaran K, Ravindran S and Venkataramani S 2002 Temporal variations in surface ozone at Thumba (8.6°N, 77°E): A tropical coastal site in India; *Atmos. Environ.* **36** 603–610, https://doi.org/10.1016/S1352-2310(01)00527-1.

Nair P R, David L M, Girach I A and George S K 2011 Ozone in the marine boundary layer of Bay of Bengal during post-winter period: Spatial pattern and role of meteorology; *Atmos. Environ.* **45**, https://doi.org/10.1016/j.atmosenv.2011.05.040.

Naja M and Lal S 2002 Surface ozone and precursor gases at Gadanki (13.5°N, 79.2°E), a tropical rural site in India; *J. Geophys. Res.* **107(D14)**, https://doi.org/10.1029/2001JD000357.

Ojha N, Naja M, Singh K P, Sarangi T, Kumar R, Lal S, Lawrence M G, Butler T M and Chandola H C 2012 Variabilities in ozone at a semi-urban site in the Indo-Gangetic Plain region: Association with the meteorology and regional processes; *J. Geophys. Res.* **117** 1–19, https://doi.org/10.1029/2012JD017716.

Panda S, Mallik C, Nath J, Das T and Ramasamy B 2021 A study on variation of atmospheric pollutants over Bhubaneswar during imposition of nationwide lockdown in India for the COVID-19 pandemic; *Air Qual. Atmos. Heal.* **14** 97–108, https://doi.org/10.1007/s11869-020-00916-5.

Schnell J L, Naik V, Horowitz L W, Paulot F, Mao J, Ginoux P, Zhao M and Ram K 2018 Exploring the relationship between surface PM2.5 and meteorology in Northern India; *Atmos. Chem. Phys.* **18** 10157–10175, https://doi.org/10.5194/acp-18-10157-2018.

Seinfeld J H and Pandis S N 1998 *Atmospheric chemistry and physics: From air pollution to climate change*; Wiley-Interscience Publication, USA.

Sharma S, Zhang M, Anshika Gao J, Zhang H and Kota S H 2020 Effect of restricted emissions during COVID-19 on air quality in India; *Sci. Total Environ.* **728** 138878, https://doi.org/10.1016/j.scitotenv.2020.138878.

Shehzad K, Sarfraz M and Shah S G M 2020 The impact of COVID-19 as a necessary evil on air pollution in India during the lockdown; *Environ. Pollut.* **266** 115080, https://doi.org/10.1016/j.envpol.2020.115080.

Singh V, Singh S, Biswal A, Kesarkar A P, Mor S and Ravindra K 2020 Diurnal and temporal changes in air pollution during COVID-19 strict lockdown over different regions of India; *Environ. Pollut.* **266** 115368, https://doi.org/10.1016/j.envpol.2020.115368.

Soni M, Ojha N and Girach I 2021 Impact of COVID-19 lockdown on surface ozone build-up at an urban site in western India based on photochemical box modelling; *Curr. Sci.* **120** 376–381, https://doi.org/10.18520/cs/v120/i2/376-381.

Tanimoto H, Mukai H, Sawa Y, Matsueda H, Yonemura S, Wang T, Poon S, Wong A, Lee G, Jung J Y, Kim K R, Lee M H, Lin N H, Wang J L, Ou-Yang C F, Wu C F, Akimoto H, Pochanart P, Tsuboi K, Doi H, Zellweger C and Klausen J 2007 Direct assessment of international consistency of standards for ground-level ozone: Strategy and implementation toward metrological traceability network in Asia; *J. Environ. Monit.* **9** 1183–1193, https://doi.org/10.1039/B701230F.

Winer A M, Peters J W, Smith J P and Pitts J N 1974 Response of commercial chemiluminescent nitric oxide-nitrogen dioxide analyzers to other nitrogen-containing compounds; *Environ. Sci. Technol.* **8** 1118–1121, https://doi.org/10.1021/es60098a004.

Corresponding editor: Parathasarathi Mukhopadhyay